Journal of Nanofluids
Vol. 5, pp. 696–706, 2016
(www.aspbs.com/jon)

ARTICLE

Effect of Aligned Magnetic Field on Slip Flow of Casson Nanofluid Over a Nonlinear Stretching Sheet with Chemical Reaction

T. Vijayalaxmi[1,2,*] and Bandari Shankar[1]

[1]*Department of Mathematics, Osmania University, Hyderabad 500007, Telangana, India*
[2]*Department of Mathematics, M. V. S. Government Arts and Science College, Mahabubnagar 509001, Telangana, India*

The numerical investigation of the flow of a Casson nanofluid over a nonlinear stretching sheet with the effects of the inclined magnetic field and chemical reaction is presented. Moreover we considered the second order thermal slip and velocity partial slip and solutal slip. The basic governing partial differential equations are converted into nonlinear ordinary differential equations by employing suitable similarity transformations. The resulting equations are successfully solved by using an implicit finite difference scheme known as Keller-Box method. Comparisons of numerical results have been done with previously published results and found in good agreement. The effects of various non dimensional parameters i.e., magnetic parameter, aligned angle, Casson parameter, second order thermal slip, velocity and solutal slip, Prandtl number, Thermophoresis parameter, Brownian motion parameter, Eckert number, Lewis number, chemical reaction parameter on velocity, temperature and concentration are discussed in detail and presented through graphs also variations of skin-friction, Nusselt and Sherwood numbers are computed and presented in tables. It is observed that the increase in aligned angle decreases the velocity profile, but it increases the temperature and concentration, the result is same in the case of Casson parameter. The first order thermal jump decreases the temperature whereas, increases the second order jump. Chemical reaction decreases the concentration profile and Nusselt, Sherwood numbers are decreases with the increase in the values of slip parameters.

KEYWORDS: Casson Fluid, Inclined Magnetic Field, Nonlinear Permeable Stretching Sheet, Partial Velocity Slip, Second Order Thermal Slip, Solutal Slip, Chemical Reaction.

1. INTRODUCTION

Casson fluid model was introduced in 1995 by Casson, is based on the interactive behaviour of a two phase suspension of solid, liquid phases and is a shear thinning liquid. It acts as a solid if the shear stress less than the yield stress applied to the fluid and behaves like a fluid if the shear stress is greater than the applied yield stress. Fluids like honey, soup, jelly, blood, food stuffs, slurries, polymeric liquids, artificial fibers are the some Casson fluids. This fluids attracted by scientist and engineers for study the fluid model and discussed its flow of boundary layer condition of various physical effects of magnetic field and slip conditions etc.[1–3] The heat, mass and momentum transfer of boundary layer near nonlinear stretching surface have received great attention during the last decades due to the various practical potential applications. In particular, chemical and manufacturing processes such as polymer extrusion, enhanced oil recovery, metal spinning, packed bed catalytic reactors, transpiration cooling, continuous casting of metals, glass and fiber production, hot rolling of paper and wire making.

The heat transfer of Casson fluid flow between rotating cylinders in the presence of a magnetic field is studied by Elbade et al.[4] A detailed work on Casson and Carreau-Yasuda non-Newtonian blood models with steady and oscillatory flow and studied its Lattice Boltzmann method to solve the governing equations by Boyd et al. in 2007.[5] Two dimensional boundary layer flow and heat transfer of Casson fluid over an unsteady stretching surface have studied by Mukhopadhyay et al.[6] Unsteady boundary layer flow of Casson fluid due to an imprudently started moving plane flat plate is studied by Mustafa.[7] The magnetohydrodynamic boundary layer flow of Casson fluid over exponentially shrinking permeable sheet is done by Nadeem.[8] In, 2012, Hayat and his group[9] studied on series solutions for MHD Casson fluid flow over a stretched surface. Sakiadis[10] reported on boundary layer flow on

*Author to whom correspondence should be addressed.
Email: vijaya9966998024@rediffmail.com
Received: 25 March 2016
Accepted: 2 May 2016

a continuously moving stretching surface. Investigations made on the heat and mass transfer over a stretching surface in different directions.[11–13] The influence of magnetic field is important in MHD generators, bearings, pumps, etc., in the boundary layer control which affected by the interaction between the magnetic field and an electrically conducting fluid. Studies have shown their interest to study the behaviour of boundary layers in the presence of a transverse magnetic field.[14, 15] The effect of inclination angle, magnetic field on flow and heat transfer of an nanofluid over impermeable stretching sheet is studied.[16] The influence of inclined Lorentz forces on boundary flow of Casson fluid over an impermeable stretching sheet with heat transfer is studied by Abdul Hakeem and his team.[17] The effect of MHD boundary layer heat and mass transfer of a chemically reacting Casson fluid over a permeable stretching surface with non-uniform heat source/sink is reported by Gireesha et al.[18] Induced magnetic field and homogeneous, heterogeneous reactions effects on stagnation flow of a Casson fluid is studied by Raju and his team.[19]

Chemical reactions are either heterogeneous or homogeneous and depend on interface or as single phase volume reactions. Chemical reaction plays vital role, and are design of chemical process equipment, formation and dispersion of fog, processing of food, and cooling towers. Flow study and chemical reaction became important in recent years. Chamkha et al.[20] studied heat and mass transfer by steady flow of an electrically conducting fluid past a moving vertical surface in presence of first order chemical reaction. Chemical reaction effects are well studies by Damseh et al.,[21] Magyari and Chamkha,[22] and Das.[23] Yazdi et al.[24] reported the MHD effect of slip flow and heat transfer over a nonlinear permeable stretching surface with chemical reaction. The heat transfer studies of mixed convection effect over a nonlinear stretching surface with variable fluid properties is studied by Prasad et al.[25] Gireesha and his team is studied the effect of magnetic filed and chemical reaction on stagnation-point flow and heat transfer of a nanofluid over an inclined stretching sheet.[26]

The steady two dimensional flow over a vertical stretching surface in presence of aligned magnetic field, cross-diffusion and radiation effects is reported by Raju et al.,[27] in which increase in aligned angle strengthen the magnetic field and decreases the velocity profile of the flow and enhances the heat transfer rate. Jing Zhu and his group studied the effects of the second order velocity slip and temperature jump boundary conditions on the magneto hydrodynamic (MHD) flow and heat transfer in the presence of nanoparticle fractions.[28]

In addition to the above importance, study of the boundary layer flows with heat transfer of a incompressible fluid over an inclined stretching surface have numerous potential applications. These are MHD power generators, flight magnetohydrodynamics, the boundary layer along a liquid film condensation process, glass and polymer industries, gas turbines, the extrusion of plastic sheets from a die, the cooling process of metallic plate in a cooling bath and as in the field of planetary magnetosphere, aeronautics and chemical engineering. Hence, the present paper addresses the effect of velocity, temperature and solutal slip flow of a Casson nanofluid over an aligned nonlinear stretching sheet in the presence of chemical reaction. Governing nonlinear ordinary differential equations obtained after the application of similarity transformations are solved numerically by means of Keller-Box method. The effects of different flow parameters on flow fields are elucidated through graphs and tables.

2. FLOW ANALYSIS AND MATHETATICAL FORMULATION

Consider the steady two dimensional flow of a viscous incompressible nanofluid over a nonlinear stretching sheet coinciding with the plane $y = 0$, with surface temperature T_w and concentration C_w. The fluid occupies the upper half plane ($y > 0$). The sheet is stretched horizontally by applying two equal and opposite forces along x-axis keeping the origin fixed. The stretching velocity of the sheet is $U_w(x) = ax^n$, where the x-component of the velocity varies non-linearly along it, $a > 0$ is constant of proportionality know as stretching rate and n is a power index. Along with these the fluid is permitted by an aligned magnetic field and also considered chemical reaction to the flow. The induced magnetic field is also assumed to be small compared to the applied magnetic field; so it is neglected. It is also assumed that the ambient fluid i.e., the fluid far away from stretching sheet is moved with velocity $U_\infty(x) = bx^n$ where $b > 0$ is a constant. The ambient temperature and concentration are respectively, $T\infty$ and $C\infty$. T is the temperature and C is the concentration of the nanofluid in the boundary layer.

We also assume that the rheological equation of extra stress tensor (τ) for an isotropic and incompressible flow of a Casson fluid[29] can be written as

$$\tau_{ij} = \begin{cases} 2(\mu_B + P_y/\sqrt{2}\pi)e_{ij}, & \pi > \pi_c \\ 2(\mu_B + P_y/\sqrt{2}\pi)e_{ij}, & \pi < \pi_c \end{cases}$$

Here μ is the dynamic viscosity and μ_B is the plastic dynamic viscosity of the non-Newtonian fluid, P_y is the yield stress of fluid, π is the product of the component of deformation rate of (i, j) the component and $\pi = e_{ij}e_{ij}$, π_c is the critical value of π based on non-Newtonian model. The governing equations for the above flow are given by

$$\frac{\partial u}{\partial x} + \frac{\partial v}{\partial y} = 0 \quad (1)$$

$$u\frac{\partial u}{\partial x} + v\frac{\partial u}{\partial y} = \nu\left(1 + \frac{1}{\beta}\right)\frac{\partial^2 u}{\partial y^2} - \frac{\sigma B^2(x)}{\rho_f}\sin^2(\theta)u \quad (2)$$

ARTICLE

$$u\frac{\partial T}{\partial x}+v\frac{\partial T}{\partial y}=\alpha\frac{\partial^2 T}{\partial y^2}+\tau\left\{D_B\frac{\partial C}{\partial y}\frac{\partial T}{\partial y}+\frac{D_T}{T_\infty}\left(\frac{\partial T}{\partial y}\right)^2\right\}+\frac{\nu}{C_p}\left(1+\frac{1}{\beta}\right)\left(\frac{\partial u}{\partial y}\right)^2 \quad (3)$$

$$u\frac{\partial C}{\partial x}+v\frac{\partial C}{\partial y}=D_B\left(\frac{\partial^2 C}{\partial y^2}\right)+\frac{D_T}{T_\infty}\left(\frac{\partial^2 T}{\partial y^2}\right)-K_r(x)(C-C_\infty) \quad (4)$$

The boundary conditions[28, 30] corresponding to the problem are as follows.

$$\begin{gathered}u=U_w+N\left(1+\frac{1}{\beta}\right)\frac{\partial u}{\partial y},\quad v=0\\ T=T_w+L_1\frac{\partial T}{\partial y}+L_2\frac{\partial^2 T}{\partial y^2}\\ C=C_w+K\frac{\partial C}{\partial y}\quad \text{at } y=0\\ u\to U_\infty,\quad v\to 0,\quad T\to T_\infty\\ C\to C_\infty\quad \text{as } y\to\infty\end{gathered} \quad (5)$$

Where u and v denotes the velocities in the direction of x-and y-respectively, β is the Casson fluid parameter, ν is the kinematic viscosity, ρ_f is the density of the base fluid, σ is the electrical conductivity, α is the thermal diffusivity, $(\rho c)_p$ is the effective heat capacity of the nano particles, $(\rho c)_f$ is the heat capacity of the base fluid, $\tau=(\rho c)_p/(\rho c)_f$ is the ratio of the nano particle heat capacity and base fluid heat capacity, D_B is the Brownian motion diffusion coefficient and D_T is the thermophoretic diffusion coefficient, $K_r(x)=2k/(a(n+1)(C_W-C_\infty))$ is the chemical reaction parameter, with rate constant K_r, where $K_r>0$ for destructive reaction, $K_r<0$ for generative reaction and $K_r=0$ for no reaction. We consider that the magnetic field $B(x)=B_0(x)x^{(n-1)/2}$, where B_0 is the constant magnetic field.

Let us introducing the following similarity transformations as

$$\begin{gathered}\eta=y\sqrt{\frac{a(n+1)}{2\nu}}x^{(n-1)/2},\quad u=ax^n f'(\eta)\\ v=-\sqrt{\frac{a\nu(n+1)}{2}}x^{(n-1)/2}\left(f(\eta)+\frac{n-1}{n+1}\eta f'(\eta)\right)\\ G(\eta)=\frac{(T-T_\infty)}{(T_w-T_\infty)},\quad H(\eta)=\frac{(C-C_\infty)}{(C_w-C_\infty)}\end{gathered} \quad (6)$$

ψ represent the stream function and is defined as $u=\partial\psi/\partial y$ and $v=-\partial\psi/\partial x$ so that Eq. (1) is satisfied identically. By employing the similarity transformations (6), the governing Eqs. (2)–(4) reduced to the following ordinary differential equations:

$$\left(1+\frac{1}{\beta}\right)f'''+ff''-\left(\frac{2n}{n+1}\right)(f')^2-Mf'\sin^2(\theta)=0 \quad (7)$$

$$G''+PrfG'+PrNbG'H'+PrNtG'^2+PrEc\left(1+\frac{1}{\beta}\right)f''^2=0 \quad (8)$$

$$H''+LefH'+\frac{Nt}{Nb}G''-RLeH=0 \quad (9)$$

By using (5) the transformed boundary conditions are:

$$\begin{gathered}f(0)=0,\quad f'(0)=1+\alpha\left(1+\frac{1}{\beta}\right)f''(0)\\ G(0)=1+\gamma G'(0)+\delta G''(0)\\ H(0)=1+\lambda H'(0)\end{gathered} \quad (10)$$

$$f(\eta)\to 0,\quad G(\eta)\to 0,\quad H(\eta)\to 0\quad \text{as } \eta\to\infty \quad (11)$$

The involved physical parameters are defined as follows:

$M=\dfrac{2\sigma B_0^2}{(n+1)a\rho_f}$ *is the magnetic parameter,*

$Pr=\dfrac{\nu}{\alpha}$ *is Prandtl number*

$Nb=\dfrac{\tau D_B(C_w-C_\infty)}{\nu}$ *is the Brownian motion parameter,*

$Nt=\dfrac{\tau D_T(T_w-T_\infty)}{T_\infty\nu}$ *is the Thermophpresis parameter,*

$Ec=\dfrac{u_w^2}{C_p(T_w-T_\infty)}$ *Eckert number,*

$\alpha=N\sqrt{\dfrac{a(n+1)}{2\nu}}x^{(n-1)/2}$ is the partial velocity slip parameter,

$\gamma=L_1\sqrt{\dfrac{a(n+1)}{2\nu}}x^{(n-1)/2}$ *and* $\delta=L_2\dfrac{a(n+1)}{2\nu}x^{n-1}$ *are the thermal jump parameters,*

$\lambda=K\sqrt{\dfrac{a(n+1)}{2}}x^{(n-1)/2}$ *is the concentration slip parameter,*

$R=\dfrac{2k}{a(n+1)(C_w-C_\infty)}x^{(n-1)/2}$ *is the chemical reaction parameter,*

$Le=\dfrac{\nu}{D_B}$ *is the Lewis number.*

The Skin friction coefficient, Nusselt number and Sherwood numbers are given by

$$C_f=\frac{\tau_w}{\rho u_w^2},\quad Nu_x=\frac{xq_w}{k(T_w-T_\infty)},\quad Sh_x=\frac{xq_m}{D_B(C_w-C_\infty)} \quad (12)$$

Here $\tau_w = \mu_B(1+1/\beta)(\partial u/\partial y)_{y=0}$, q_w, and, q_m are the heat and mass fluxes at the surface respectively are given by

$$q_w = -k\left(\frac{\partial T}{\partial y}\right)_{y=0}, \quad q_m = -D_B\left(\frac{\partial C}{\partial y}\right)_{y=0} \tag{13}$$

where k is thermal conductivity of the nanofluid.

By substituting Eq. (6) into Eqs. (12)–(13), we will get

$$\begin{aligned} C_f Re^{1/2} &= \left(1+\frac{1}{\beta}\right)f''(0) \\ Nu_x Re^{-1/2} &= -G'(0) \\ Sh_x Re^{-1/2} &= -H'(0) \end{aligned} \tag{14}$$

where $Re = (u_w x(n+1))/2$ local Reynolds number.

3. NUMERICAL METHODS

The non linear ordinary differential Eqs. (7)–(9) together with boundary conditions (10)–(11) are solved numerically by an implicit finite difference scheme namely the Keller box method as mentioned by Cebeci and Bradshaw.[31] According to Vajravelu et al.,[32] to obtain the numerical solutions, the following steps are involved in this method.

- Reduce the ordinary differential equations to a system of first order equations.
- Write the difference equations for ordinary differential equations using central differences.
- Linearize the algebraic equations by Newtons method, and write them in matrix vector form.
- Solve the linear system by the block tri-diagonal elimination technique.

The accuracy of the method is depends on the appropriate initial guesses. We made an initial guesses are as follows.

$$f_0(\eta) = \frac{1}{1+(1+1/\beta)\alpha}(1-e^{-x})$$

$$G_0(\eta) = \left(\frac{1}{1+\gamma-\delta}\right)e^{-x}, \quad H_0(\eta) = \left(\frac{1}{1+\lambda}\right)e^{-x}$$

The choices of the above initial guesses depend on the convergence criteria and the transformed boundary conditions of Eqs. (10) and (11). The step size 0.01 is used to obtain the numerical solution with four decimal place accuracy as the criterion of convergence.

4. RESULTS AND DISCUSSION

The theme of this section is to discuss the effects of various physical parameters such as magnetic parameter M, Casson fluid parameter β, aligned angle θ, partial velocity slip parameter α, thermal jump parameters γ and δ, concentration slip λ, nonlinearity parameter n, Prandtl number Pr, thermophoresis parameter Nt, Brownian motion parameter Nb, Eckert number Ec, Lewis number Le, chemical reaction parameter R on the velocity profile $f'(\eta)$, temperature profile $-G'(\eta)$ and concentration profile $-H'(\eta)$.

To validate the present results, comparisons have been made with previous results in the absence of nanofluid, slip effects, chemical reaction and Casson fluid parameter for $-(1+1/\beta)f"(0), -G'(0), -H'(0)$ presented in Table I and which are found in good agreement with previous studies.[33]

Figures 1–13 depicts the graphical representations of the various controlling parameters on the velocity, temperature and concentration profiles. Effect of magnetic parameter M on the velocity profile is displayed in Figure 1 by keeping the other parameters fixed. It is observed that an increase in magnetic field parameter decreases the

Table I. Comparison of Skin friction coefficient, Nusselt and Sherwood numbers when $\alpha=\beta=\gamma=\delta=R=\lambda=\theta=0$.

Ec	M	$-f''(0)$ (Mabood et al.,[33])	$-f''(0)$ (Present)	$-G'(0)$ (Mabood et al.,[43])	$-G'(0)$ (Present)	$-H'(0)$ (Mabood et al.,[33])	$-H'(0)$ (Present)
0	0	1.10102	1.1010	1.06719	1.0672	1.07719	1.0772
0.1				0.88199	0.8892	1.22345	1.2234
0.2				0.70998	0.7100	1.37078	1.3708
0.3				0.52953	0.5295	1.51919	1.5192
0.5				0.16484	0.1648	1.81933	1.8194
0	0.5	1.3098	1.3099	1.04365	1.0473	1.01090	1.0109
0.1				0.81055	0.8106	1.20605	1.2060
0.2				0.57564	0.5757	1.40279	1.4028
0.3				0.33889	0.3389	1.60115	1.6012
0.5				0.14022	0.1402	2.00282	2.0028
0	1	1.48912	1.4891	1.02337	1.0234	0.95495	0.9549
0.1				0.74058	0.7406	1.19496	1.1950
0.2				0.45543	0.4554	1.43706	1.4371
0.3				0.16789	0.1679	1.68128	1.6813
0.5				0.41451	0.4145	2.17623	2.1763

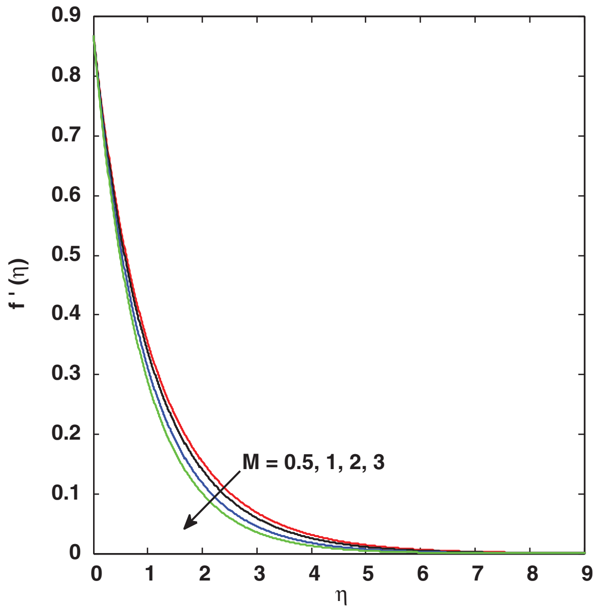

Fig. 1. Effect of magnetic parameter (M) on velocity profile.

velocity. Increasing magnetic field parameter improves the opposite force to the flow of nanofluid direction called 'Lorentz force'. This Lorentz force opposes the motion of the nanofluid which results in decreases the velocity of the fluid. The Figure 1 represent the velocity of the nanofluid reduces, as the magnetic field parameter M increases.

Figure 2(a) represents the influence of Casson parameter β on the velocity profile. From the Figure, we can observe that increase in the values of Casson fluid parameter, the velocity distribution of the fluid is reduced inside the boundary layer away from the surface but reverse is true along the surface, the yield stress is decreasing with an increase in Casson parameter. Due to this the resistance force occurred and it makes the fluid velocity reduces. The variation in temperature profile for variable values of Casson parameter is presented in Figure 2(b). It is evident from the Figure the temperature distribution is found to increase along the thermal boundary layer with the larger values of the Casson fluid parameter. The thermal boundary layer thickness increases with increasing the Casson parameter. Which gives the heat transfer rate at the surface is decreases, so, the temperature on the surface of the sheet increases. Due to the inversely proportionality of heat transfer coefficient to thermal resistance and the directly proportionality of the Casson parameter to heat transfer coefficient, the convection resistance on the hot side of the fluid decreases so the surface temperature increases as Casson parameter increases.

Figures 3(a–c) are plotted to observe the effects of angle of inclination θ on velocity, temperature and concentration profiles respectively. It is clear from figures that the temperature and concentration profiles are increased with increase in inclined angle, this enhancement is due to the raise in the magnetic field parameter. The velocity profile decreases with the increase of aligned angle. It may happen with the increase in angle of inclination, causes to strengthen the applied magnetic field. Because of enhanced magnetic field an opposite force is produced to the flow, called Lorentz force. Consequently the velocity profile decreases. It is also seen that for the angle $\theta = 0$ the magnetic field is not effected on the velocity profile while maximum resistance is offered for the fluid particles when $\theta = \pi/2$.

The effects of partial velocity slip parameter on the dimensionless velocity $f'(\eta)$ and temperature $-G(\eta)$ is displayed in Figures 4(a and b) respectively. From the Figures velocity decreases with increase in the values of slip parameter, velocity distribution is found to decrease along the boundary layer, but it is reverse in the case of temperature, i.e., temperature increases with the increase

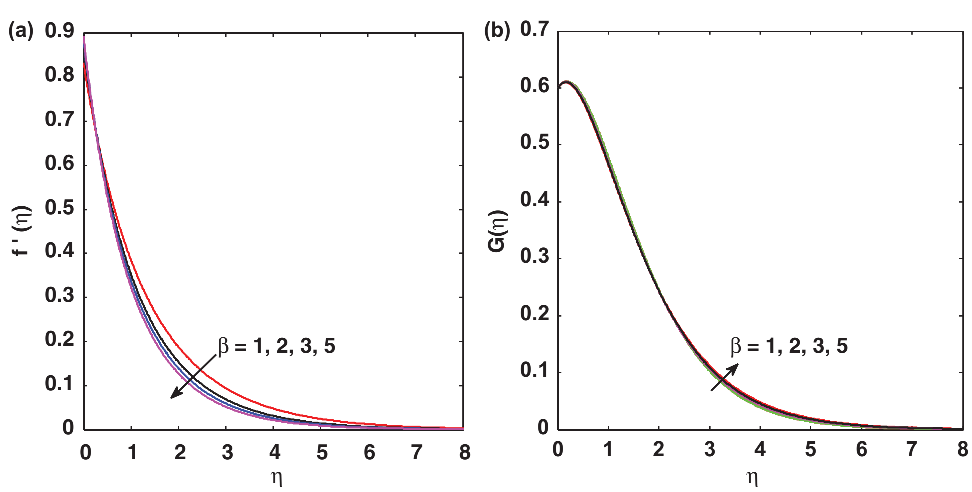

Fig. 2. (a) Effect of Casson parameter (β) on velocity profile. (b) Effect of Casson parameter (β) on temperature profile.

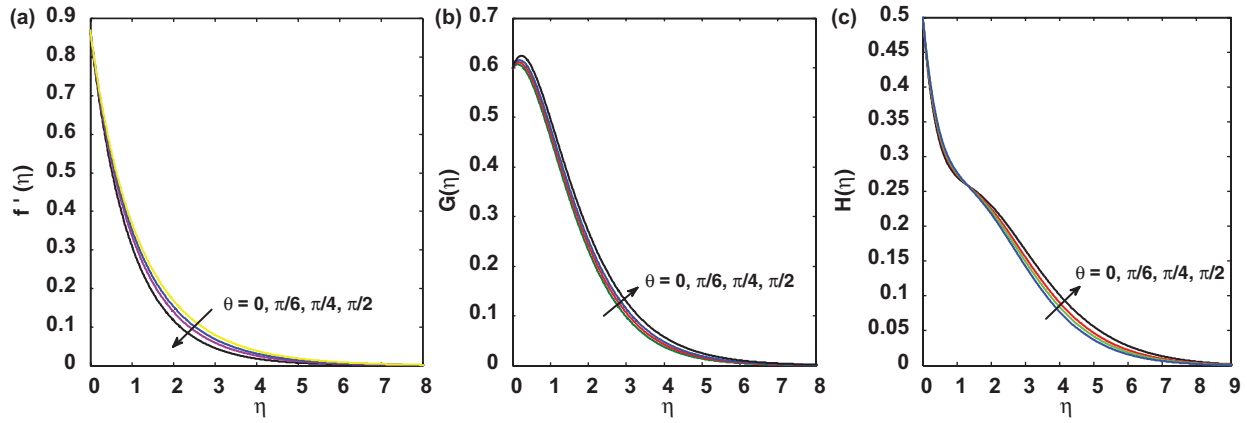

Fig. 3. (a) Effect of inclined angle (θ) on velocity profile. (b) Effect of inclined angle (θ) on temperature profile. (c) Effect of inclined angle (θ) on concentration profile.

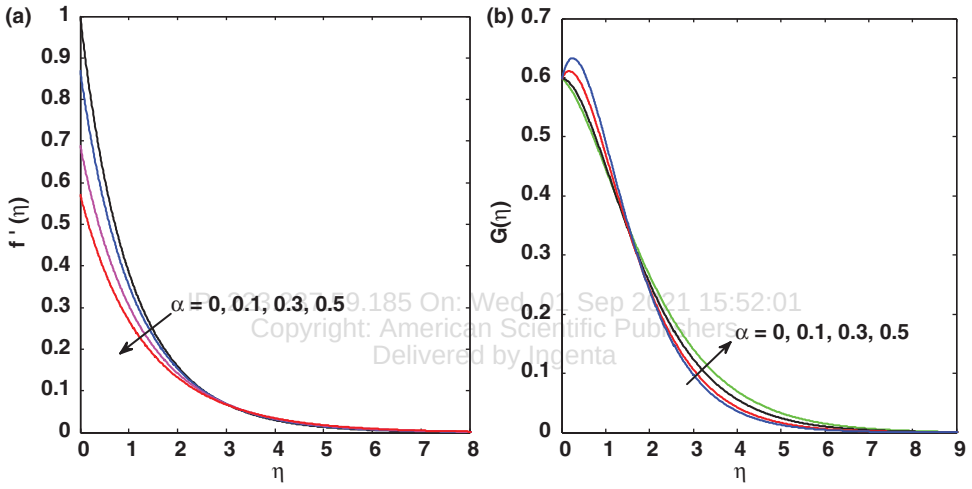

Fig. 4. (a) Effect of velocity partial slip (α) on velocity profile. (b) Effect of velocity partial slip (α) on temperature profile.

of partial slip parameter. Physically, in the presence of slip the slipping fluid shows a decrease in the surface skin-friction between the stretching sheet and the fluid because not all the pulling force of the stretching surface can be transferred to the fluid. So the flow velocity decreases when the value of α increases. As the slip parameter increases in magnitude the friction force is occurred which allows more fluid to slip past the sheet, the flow slows down for distances close to the sheet and the temperature enhances due to the occurrence of the force. On observing from Figure 5, as the nonlinear parameter increases, the velocity profile decreases.

The influence of thermal jump parameters γ and δ on the temperature profiles is shown in Figures 6(a and b) which describes that the fluid temperature decreases on increasing thermal jump parameters in the boundary layer region. As the effect increases more fluid will be transferred to the thermal boundary layer. Hence, rate of heat transfer will increase and as a result of this, the thermal boundary layer decreases.

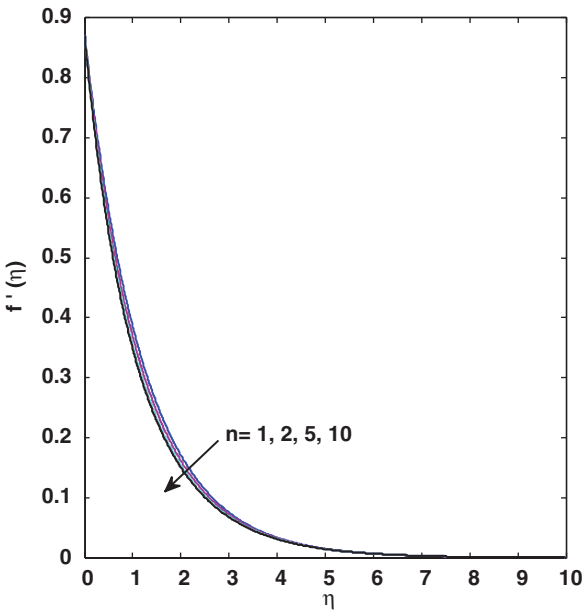

Fig. 5. Effect of nonlinear parameter (n) on velocity profile.

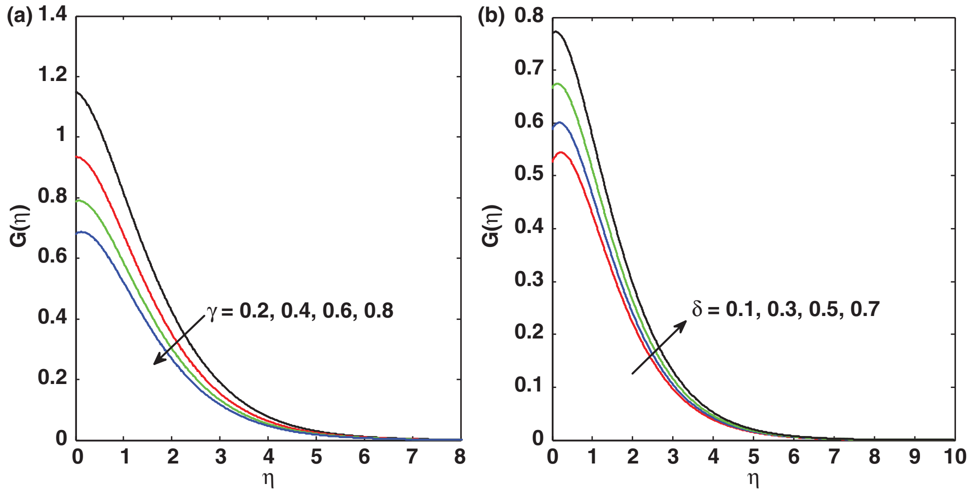

Fig. 6. (a). Effect of temperature jump (γ) on temperature profile. (b). Effect of temperature jump (δ) on temperature profile.

From Figure 7 we can observe the variation of concentration with respect to solutal slip parameter λ. As it can be seen from the graph, increasing in the concentration slip parameter λ, the concentration profile is decreasing.

The effect of Prandtl number Pr on the heat transfer process is shown by the Figure 8. This figure reveals that as an increase in Prandtl number Pr, the temperature field decreases. An increase in the values of Pr reduces the thermal diffusivity, because Prandtl number is a dimensionless number which is defined as the ratio of momentum diffusivity to thermal diffusivity, that is $Pr = \upsilon/\alpha$. Increasing the values of Pr implies that momentum diffusivity is higher than thermal diffusivity. Therefore thermal boundary layer thickness is a decreasing function of Pr.

The influence of Eckert number Ec is depicted in Figure 9. It illustrates that the temperature increases with an increase in Ec. The viscous dissipation produces heat due to drag between the fluid particles and this extra heat causes an increase of the initial fluid temperature.

The effect of Brownian motion parameter Nb on temperature and concentration are presented in Figures 10(a and b). The Figure 10(a) represents the variation of temperature with the Brownian motion parameter Nb. Increase in Nb values gives the temperature graph decrease and increase in thermal boundary layer thickness. As increase in Nb, due to movement of nanoparticles,

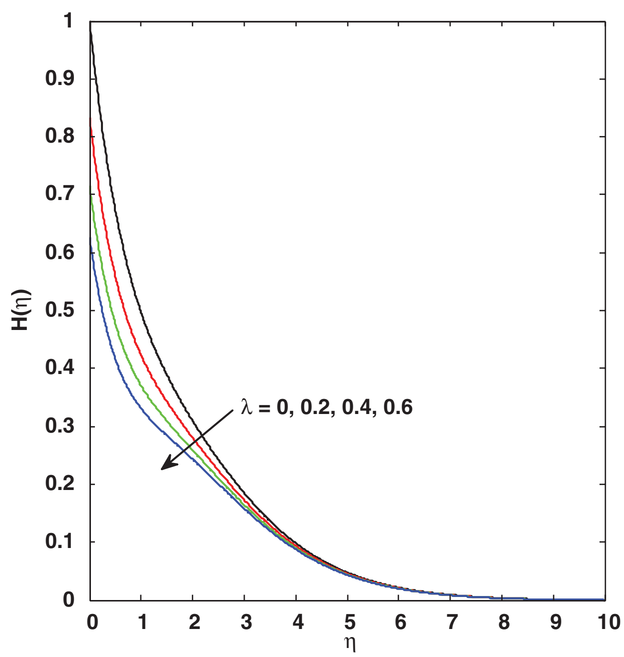

Fig. 7. Effect of solutal slip (λ) on concentration profile.

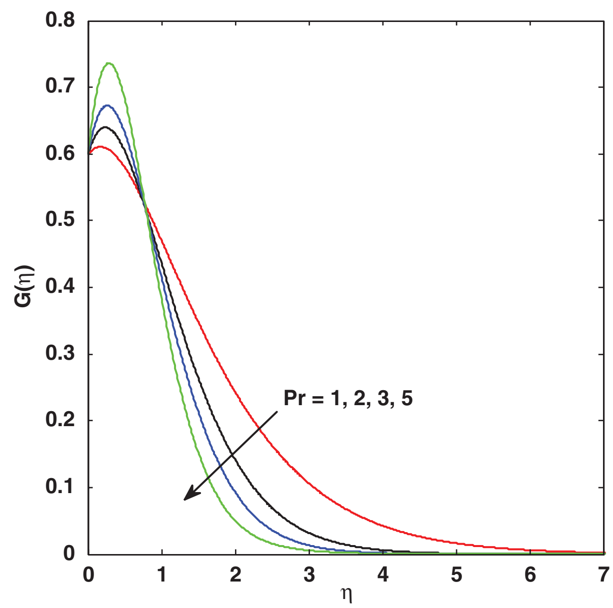

Fig. 8. Effect of Prandtl number (Pr) on temperature profile.

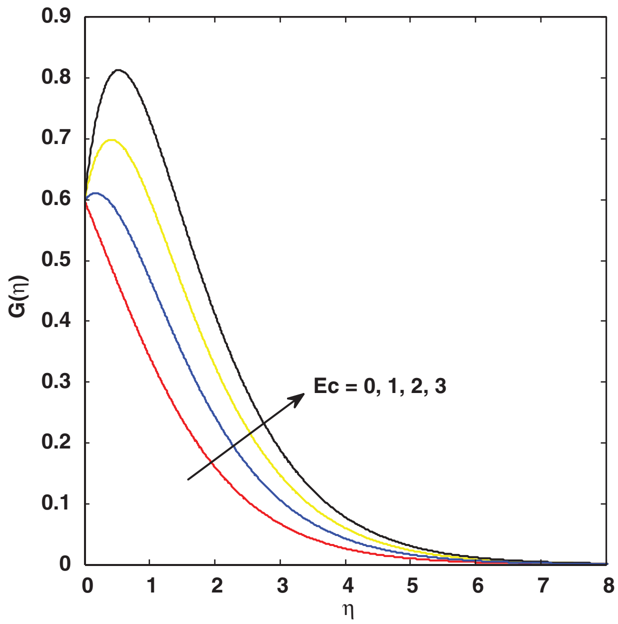

Fig. 9. Effect of Eckert number (Ec) on temperature profile.

results in increase the kinetic energy of the nanoparticle, thus rises the temperature. But it is reverse in the case of nano particle volume fraction profile, i.e., as the values of Nb increase, the concentration boundary layer thickness decrease.

Figures 11(a and b) shows the impact of thermophoresis parameter Nt on temperature and nanoparticle concentration profile respectively. It is found that an increase in the thermophoresis parameter Nt leads to increase in both temperature and nanoparticle concentration. As the thermophoretic effect increases, nanoparticles are migrated from the hot surface to cold ambient fluid, as a result the temperature enhanced in the boundary layer. This will helps in the thickening of the thermal boundary layer. Figure 11(b) reveals the variation of concentration profile and it can be seen from the graph concentration profile is monotic. As the larger thermophoresis parameter Nt values gives the larger temperature gradient. The concentration field is motivated by the temperature gradient with the temperature is an increasing function of Nt, an increase in Nt parameter increases the concentration and its boundary layer thickness. The nanoparticle concentration increases, as the Nt and concentration boundary layer thickness increases.

Figure 12 shows the impact of Lewis number Le on concentration profile. Actually, a higher value of Lewis number $Le = \alpha/D_B$ represents a lower nanoparticle diffusivity (Brownian motion) and a higher thermal diffusivity. If $Le > 1$, the thermal diffusion rate exceeds the Brownian diffusion rate. Lower Brownian diffusion leads to less mass transfer rate, as a result, the nanoparticle volume fraction (concentration) graph and the concentration boundary layer thickness decrease.

Figure 13 illustrates the effect of chemical reaction parameter on dimensionless nanoparticle concentration. It is observed that the nanoparticle volume fraction decreases with the increase of chemical reaction parameter whereas the parameter shows no substantial changes on dimensionless velocity and dimensionless temperature profiles.

Table II is presented to get clear insight of the skin-friction coefficient, with variable values of magnetic parameter M, nonlinearity parameter n, Casson parameter β, partial velocity slip parameter α, aligned angle θ. From this table it is observed that the skin-friction coefficient is increases when magnetic parameter, nonlinear parameter and inclined angle increases. However increase in the values of partial velocity slip parameter, Casson parameter decreases the skin-friction.

Table III illustrates the variations of Nusselt number $-G'(0)$ with variable values of M, β, α, Ec, Pr, γ, δ,

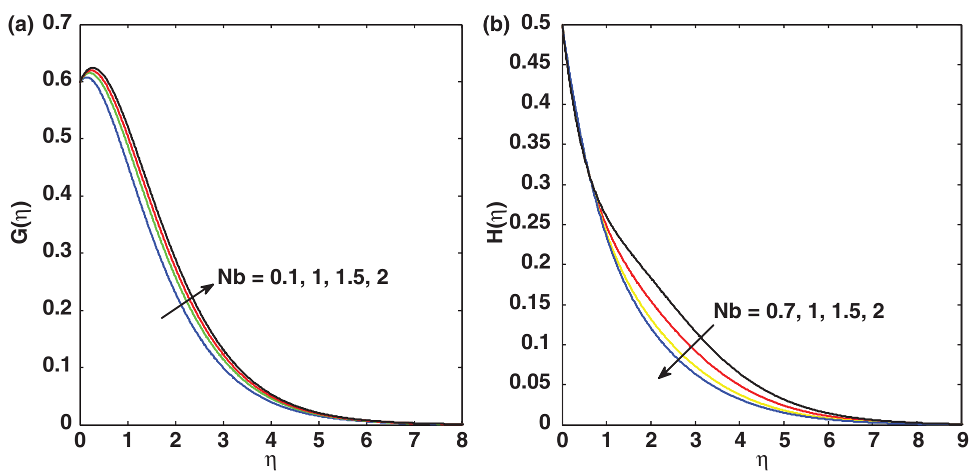

Fig. 10. (a) Effect of Brownian motion parameter (Nb) on temperature profile. (b) Effect of Brownian motion parameter (Nb) on concentration profile.

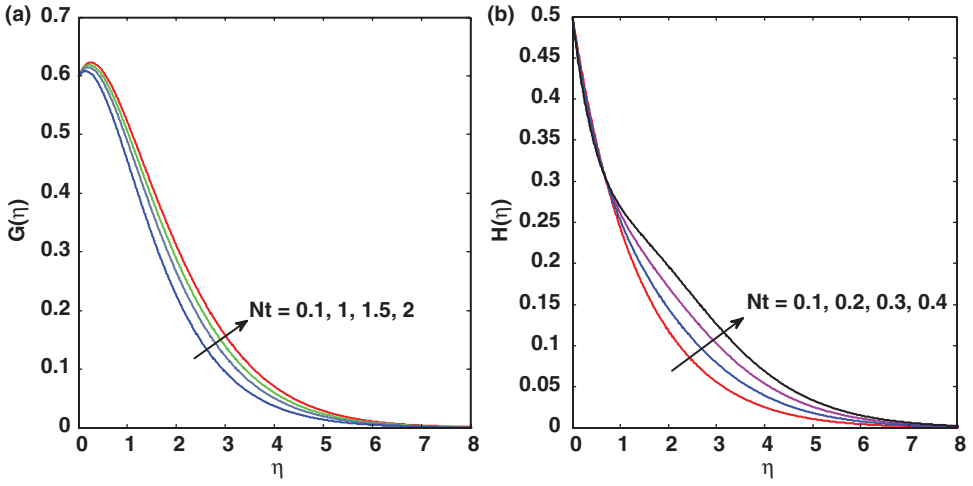

Fig. 11. (a) Effect of Themophoresis parameter (Nt) on temperature profile. (b) Effect of Themophoresis parameter (Nt) on concentration profile.

Nb and Nt. From the table it is clear that increase in the values of the partial slip parameter, first order thermal slip parameter reduces the Nusselt number. Nusselt number is increased with increase the values of both Prandtl number and second order thermal jump, also the result is same in the case of Nt, Nb when these values are increasing.

Table IV shows the Sherwood number $-H'(0)$ for different values of Lewis number Le, thermophoresis parameter Nt, Brownian motion parameter Nb, chemical reaction parameter R and solutal slip parameter λ by fixing other parameters. From this we can conclude that Sherwood number is reduced with increasing the values of Nt while increases with increasing the values of Le, Nb, R and chemical reaction parameter λ.

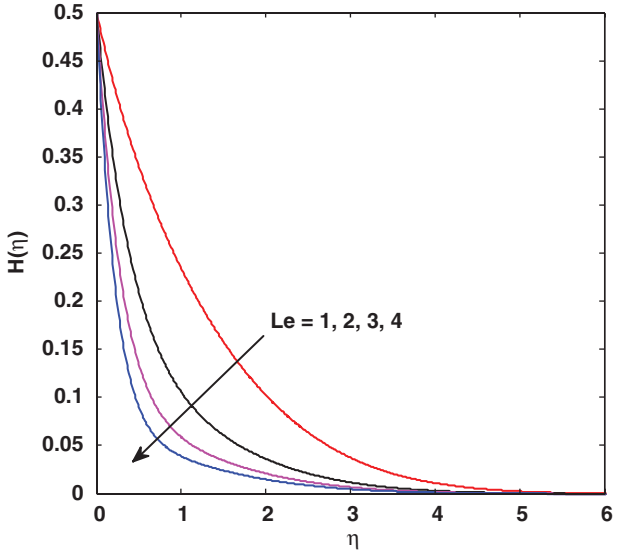

Fig. 12. Effect of Lewis number (Le) on concentration profile.

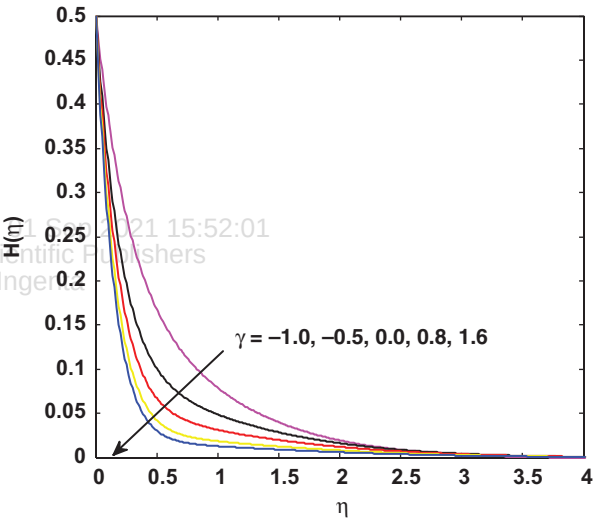

Fig. 13. Effect of chemical reaction parameter (γ) on concentration profile.

Table II. Calculation of skin friction coefficient for various values of Gr, Gc, λ, M, s, A, B.

M	N	β	α	θ	$-f''(0)$
0.5	5	1	0.1	$\pi/6$	0.6760
1.0					0.7077
1.5					0.7380
	0.5				0.5213
	1.5				0.6082
	3.0				0.6525
		0.5			0.4916
		1.5			0.7714
		2.0			0.8303
			0.5		0.3242
			1.0		0.1830
			2.0		0.0909
				$\pi/6$	0.6760
				$\pi/4$	0.7077
				$\pi/2$	0.7671

Table III. Calculation of Nussult for various values of Pr, R, Ec, Gr, Q, C.

M	β	α	Ec	Pr	γ	δ	Nb	Nt	$-G'(0)$
0.5	1	0.2	1	2	1	0.33	0.1	0.1	−0.0922
1									−0.1381
1.5									−0.1819
	0.5								−0.0181
	1.5								−0.1188
	2								−0.1317
		0.5							0.1365
		1							0.2041
		2							0.1931
			1						−0.0922
			2						−0.6206
			3						−1.1564
				1					0.0022
				3					−0.2005
				5					−0.4242
					0.5				0.0840
					1				−0.0922
					2				−0.2522
						0.1			−0.1433
						0.5			−0.0448
						0.7			0.0259
							0.2		−0.1050
							0.3		−0.1168
							0.4		−0.1278
								0.2	−0.1045
								0.3	−0.1164
								0.4	−0.1278

Table IV. Calculation of Sherwood numbers for various values of Le, Nb, Nt, R, λ.

Le	Nb	Nt	R	λ	$-H'(0)$
1					0.5087
4					0.8997
7					1.1353
	0.2				0.6903
	0.3				0.6351
	0.4				1.0418
		0.2			1.5676
		0.3			0.8729
		0.4			0.9939
			0.2		1.0932
			0.4		1.3806
			0.6		0.6055
				0	
				2	0.6055
				4	0.5085

5. CONCLUSIONS

The numerical study of the flow of a Casson nanofluid over a nonlinear stretching sheet with the effects of inclined magnetic field, chemical reaction along with the partial velocity slip, thermal jump and solutal slip has been presented in this paper. The governing partial differential equations are converted into nonlinear ordinary differential equation by employing suitable similarity transformations and solved numerically by an implicit finite difference method known as Keller-Box method. It has been presented the influence of various governing parameters on velocity, temperature and concentration profiles and illustrated graphically. The main results of this numerical study are summarized as follows.

- Increase in magnetic field M, leads to presence of Lorentz force, due to this effect it decelerates the velocity.
- Due to the rise in the inclined angle θ make stronger the magnetic field therefore velocity profile decreases.
- Increasing the value of Casson parameter leads to decrease in velocity profile but it is reverse in the case of temperature profile i.e., temperature is enhanced with the increase of Casson parameter.
- The velocity of the fluid decreases with an increase in nonlinear stretching parameter.
- When the partial velocity slip parameter α increases the velocity profile decreases.
- Temperature profile reduces with an increase in values of thermal jump parameters and Prandtl number Pr.
- The temperature increases with an increase in Eckert number.
- As the thermophoresis parameter increases both temperature and concentration profile increases.
- Temperature profile increases with increase in Brownian motion parameter but concentration profile decreases.
- Concentration profile is a decreasing function of Lewis number and chemical reaction parameter.
- Concentration profile decreases with an increase in concentration slip parameter λ.

Acknowledgments: The author T. Vijayalaxmi grateful to University Grants Commission (UGC), India for awarding Faculty Development Programme (FDP) and also thankful to CCE, Government of Telangana State and Principal, M. V. S. Government Arts and Science College, Mahabubnagar, Telangana State.

References and Notes

1. S. Mukhopadhyaym and K. Vajravelu, *J. Hydrodynam. Sr. B* 25, 591 **(2013)**.
2. S. Nadeem, R. U. Haq, N. S. Akbar, and Z. H. Khan, *Alexandria Eng. J.* 52, 577 **(2013)**.
3. M. H. Abolbashari, N. Freidoonimehr, F. Nazari, and M. M. Rashidi, *Adv. Power Technol.* 26, 542 **(2015)**.
4. N. T. M. Elbade and M. G. E. Salwa, *J. Phy., Soc. Jpn.* 64, 41 **(1995)**.
5. J. Boyd, J. M. Buick, and S. Green, *Phys. Fluids* 19, 93 **(2007)**.
6. S. Mukhopadhyay, P. Ranjan De, K. Bhattacharyya, and G. C. Layek, *Ain Shams Eng. J.* 4, 933 **(2013)**.
7. M. Mustafa, T. Hayat, I. Pop, and A. Aziz, *Heat Transfers-Asian Resc.* 40 563 **(2011)**.
8. S. Nadeem, R. UlHaq, and C. Lee, *Scientia Iranica.* 19, 1550 **(2012)**.
9. T. Hayat, S. A. Shehzad, and A. Alsaedi, *Appl. Math. Mech.* 33, 1301 **(2012)**.
10. B. C. Sakiadis, *A. I. Ch. E. J.* 7, 26 **(1961)**.
11. L. J. Crane, *Angew. Math. Phys.* 21, 645 **(1970)**.

12. R. Cortell, *Appl. Math. Compt.* 168, 557 **(2005)**.
13. F. K. Tsou, E. M. Sparrow, and R. J. Goldstein, *Int. J. Heat Mass Transfer.* 10, 219 **(1967)**.
14. A. Ishak, K. Jafar, N. Nazar, and I. Pop, *Phys. A* 388, 3377 **(2009)**.
15. H. R. Ashorynejad, M. Sheikholeslami, I. Pop, and D. D. Ganji, *Heat Mass Transfer.* 49, 427 **(2013)**.
16. N. G. Rudraswamy and B. J. Gireesha, *J. Nanofluids* 3, 181 **(2014)**.
17. A. K. Abdul Hakeem, P. Renuka, N. Vishnu Ganesh, R. Kalaivanan, and B. Ganga, *J. Mag. Mag. Mat.* 401, 354 **(2016)**.
18. B. J. Gireesha, B. Mahanthesh, and M. M. Rashidi, *Int. J. Industrial Mathematics* 7, 247 **(2015)**.
19. C. S. K. Raju, N. Sandeep, and S. Saleem, *Eng. Sci. Tech. I. J.* 19, 875 **(2016)**.
20. A. J. Chamkha, *Int. Commun Heat Mass Transfer.* 30, 413 **(2003)**.
21. R. A. Damseh, M. Q. Al-Oda, and A. J. Chamkha, *Int. J. Therm. Sci.* 48, 1658 **(2009)**.
22. E. Magyari and A. J. Chamkha, *Int. J. Therm. Sci.* 49, 1821 **(2010)**.
23. K. Das, *Int. J. Heat Mass Transfer.* 54, 3505 **(2011)**.
24. M. H. Yazdi, S. Abdullah, and I. Hashim, *Int. J. Heat Mass Transfer.* 54, 3214 **(2011)**.
25. K. V. Prasad, K. Vajravelu, and P. S. Datti, *Int. of Non-Linear Mech.* 45, 320 **(2010)**.
26. N. G. Rudraswamy, B. J. Gireesha, and A. J. Chamkha, *J. Nanofluids* 4, 239 **(2015)**.
27. C. S. K. Raju, N. Sandeep, C. Sulochana, V. Sugunamma, and M. Jayachandra Babu, *J. Nigerian Math. Soc.* 34, 169 **(2015)**.
28. J. Zhu, L. Zheng, L. Zheng, and X. Zhang, *Appl. Math. Mech.-Engl. Ed.* 36, 1131 **(2015)**.
29. T. Hayat, S. A. Shehzad, and A. Alsaedi, *Appl. Math. Mech.* 33, 1301 **(2012)**.
30. W. Ibrahim and O. D. Makinde, *J. Aerospace Eng.* 29, 04015037 **(2015)**.
31. T. Cebeci and P. Bradshaw, Physical and Computational Aspects of Convective Heat Transfer, Springer, New York, USA **1988**.
32. K. Vajravelu, K. V. Prasad, and C.-O. Ng, *Real World Appl.* 14, 455 **(2013)**.
33. F. Mabood, W. A. Khan, and A. I. M. Ismail, *J. Mag. Mag. Mat.* 374, 569 **(2015)**.